JOURNAL OF GEOPHYSICAL RESEARCH, VOL. 112, B10212, doi:10.1029/2006JB004730, 2007

Effects of Fe spin transition on the elasticity of (Mg, Fe)O magnesiowüstites and implications for the seismological properties of the Earth's lower mantle

S. Speziale,[1,5] V. E. Lee,[1] S. M. Clark,[2] J. F. Lin,[3] M. P. Pasternak,[4] and R. Jeanloz[1]

Received 1 September 2006; revised 30 June 2007; accepted 25 July 2007; published 31 October 2007.

[1] High-pressure x-ray diffraction of $(Mg_{0.80}Fe_{0.20})O$ at room temperature reveals a discontinuity in the bulk modulus at 40 (±5) GPa, similar to the pressure at which an electronic spin-pairing transition of Fe^{2+} is observed by Mössbauer spectroscopy. We determine the zero-pressure bulk modulus of low-spin magnesiowüstite to be between K_{T0} = 136 and 246 GPa, with a pressure derivative $(\partial K_T/\partial P)_{T0}$ between 5.2 and 3.9. The best fit unit-cell volume at zero pressure, V_0 = 71 (±5) Å^3, is consistent with past estimates of the ionic radius of octahedrally-coordinated low-spin Fe^{2+} in oxides. A spin transition at lower-mantle depths between 1100 and 1900 km (40–80 GPa) would cause a unit-cell volume decrease (ΔV) of 3.7 (±0.5) to 2.0 (±0.1) percent and bulk sound velocity increase (Δv_ϕ) of 7.6 (±4) percent at 40 GPa and 7.6 (±1.2) percent at 80 GPa. Even in the absence of a visible seismic discontinuity, we expect the spin transition of iron to imply a correction to current compositional models of the lower mantle, with up to 10 mol percent increase of magnesiowüstite being required to match the seismological data.

Citation: Speziale, S., V. E. Lee, S. M. Clark, J. F. Lin, M. P. Pasternak, and R. Jeanloz (2007), Effects of Fe spin transition on the elasticity of (Mg, Fe)O magnesiowüstites and implications for the seismological properties of the Earth's lower mantle, *J. Geophys. Res.*, *112*, B10212, doi:10.1029/2006JB004730.

1. Introduction

[2] The behavior of ferrous iron (Fe^{2+}) in the oxide minerals of the Earth's deep interior has long attracted attention because of the importance of this transition element in influencing chemical partitioning and reactions among mantle minerals and with core material, as well as thermal, electrical, and mechanical properties at depth [e.g., *Fyfe*, 1960; *Burns*, 1970; *Gaffney and Anderson*, 1973; *Sherman*, 1988; *Cohen et al.*, 1997; *Lin et al.*, 2005; *Goncharov et al.*, 2006; *Lin et al.*, 2006; *Keppler et al.*, 2007]. Mg-rich magnesiowüstite with a composition between $(Mg_{0.9}Fe_{0.1})O$ and $(Mg_{0.6}Fe_{0.4})O$ is expected to be the second most abundant mineral of the Earth's lower mantle, after (Mg, Fe)SiO_3 perovskite. However, because of its simpler composition and crystal structure and its higher Fe content one expects that the properties of magnesiowüstite can be especially sensitive to the electronic properties of iron. Electronic transitions at the conditions of the Earth's deep interior also have the potential to strongly affect the static structure and dynamics, and hence the evolution of our planet.

[3] In recent years, the pressure-induced transition of Fe from high-spin (HS; or spin unpaired) to low-spin (LS; or spin paired) has been experimentally observed in the MgO-FeO solid solution series by means of several experimental techniques [*Pasternak et al.*, 1997; *Badro et al.*, 1999, 2003; *Lin et al.*, 2005; *Speziale et al.*, 2005; *Lin et al.*, 2006a; *Kantor et al.*, 2006a]. The emerging picture from recent experimental and theoretical results is that the pressure at which the HS to LS transition begins increases with increasing FeO content, from between 40 and 60 GPa for 10 mol% FeO to above 80–90 GPa for Fe-rich compositions and FeO (Figure 1) [*Pasternak et al.*, 1997; *Struzhkin et al.*, 2001; *Badro et al.*, 1999, 2003; *Lin et al.*, 2005, 2006a; *Speziale et al.*, 2005; *Kantor et al.*, 2006a, 2007; *Tsuchiya et al.*, 2006; *Persson et al.*, 2006].

[4] Both *Lin et al.* [2005] and *Speziale et al.* [2005] have independently analyzed x-ray diffraction spectra in combination with separate determinations of the spin state of Fe in (Mg, Fe)O, by x-ray emission spectroscopy or Mössbauer spectroscopy, respectively. Here we consider the results for $(Mg_{0.80}Fe_{0.20})O$ [*Speziale et al.*, 2005], combining them with those for $(Mg_{0.83}Fe_{0.17})O$ by *Lin et al.* [2005] to obtain constraints on the equation of state of the low-spin phase.

2. Experiment

[5] Our data are the results of room temperature synchrotron X-ray diffraction measurements on polycrystalline

[1]Department of Earth and Planetary Science, University of California, Berkeley, California, USA.
[2]Advanced Light Source, Lawrence Berkeley National Laboratory, Berkeley, California, USA.
[3]Lawrence Livermore National Laboratory, Livermore, California, USA.
[4]School of Physics and Astronomy, Tel Aviv University, Tel Aviv, Israel.
[5]Now at GeoForschungsZentrum Potsdam, Telegrafenberg, Potsdam, Germany.

0148-0227/07/2006JB004730$09.00

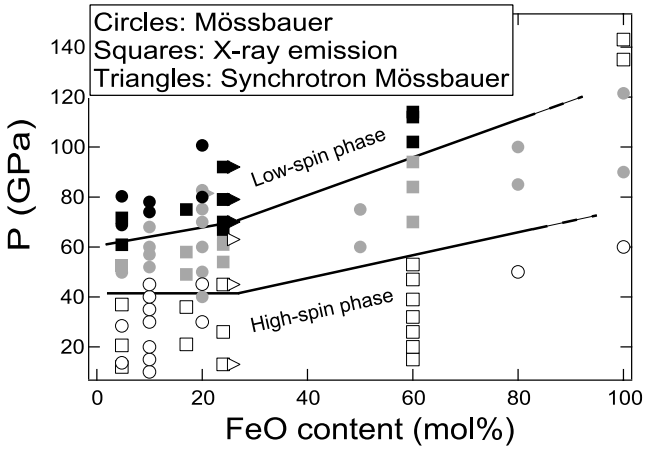

Figure 1. Phase diagram indicating the electron-spin transition of Fe^{2+} in magnesiowüstite as a function of pressure and composition: open and closed symbols indicate high-spin and low-spin states, respectively, and grey symbols indicate coexisting spin states (data from *Pasternak et al.* [1997]; *Badro et al.* [1999, 2003]; *Lin et al.* [2005, 2006a, 2007b]; *Speziale et al.* [2005]; *Kantor et al.* [2006a, 2007] and, for $Mg_{0.90}Fe_{0.10}O$, from unpublished work of Pasternak). Lines indicate onset and completion of the high-spin to low-spin transition.

$(Mg_{0.80}Fe_{0.20})O$ [*Speziale et al.*, 2005] and $(Mg_{0.83}Fe_{0.17})O$ [*Lin et al.*, 2005] compressed in gasketed diamond-anvil cells. The measurements on $(Mg_{0.8}Fe_{0.2})O$ were performed at beamline 12.2.2 of the Advanced Light Source, Lawrence Berkeley National Laboratory [*Kunz et al.*, 2005], with additional measurements performed at beamline 13ID-D of the GSECARS (GeoSoilEnviro CARS) and at 16ID-B of the HPCAT (High-Pressure Collaborative Access Team) of the Advanced Photon Source, Argonne National Laboratory; these samples were loaded in a methanol–ethanol–water mixture (16:3:1 volume ratio) or argon as pressure-transmitting media and annealed up to 450 K for about 30 min after each pressure increase. All the measurements on $(Mg_{0.83}Fe_{0.17})O$ were performed at the HPCAT of the Advanced Photon Source, Argonne National Laboratory; this sample was loaded in a neon pressure medium with platinum as the pressure calibrant, and was not annealed at high pressures. Both $(Mg_{0.80}Fe_{0.20})O$ and $(Mg_{0.83}Fe_{0.17})O$ sample material had Fe^{3+} content below the detection level of Mössbauer spectroscopy, $Fe^{3+}/(Fe^{2+}+Fe^{3+})<0.01$ [*Lin et al.*, 2005; *Speziale et al.*, 2005]. Further experimental details have been given by *Speziale et al.* [2005] and *Lin et al.* [2005].

3. Results and Discussion

[6] We have determined the unit-cell parameters of $(Mg_{0.80}Fe_{0.20})O$ from x-ray diffraction patterns of a mixture of $(Mg_{0.80}Fe_{0.20})O$ and $(Mg_{0.10}Fe_{0.90})O$, [cf. *Speziale et al.*, 2005] collected up to 62 GPa (Figure 2). The Fe-rich

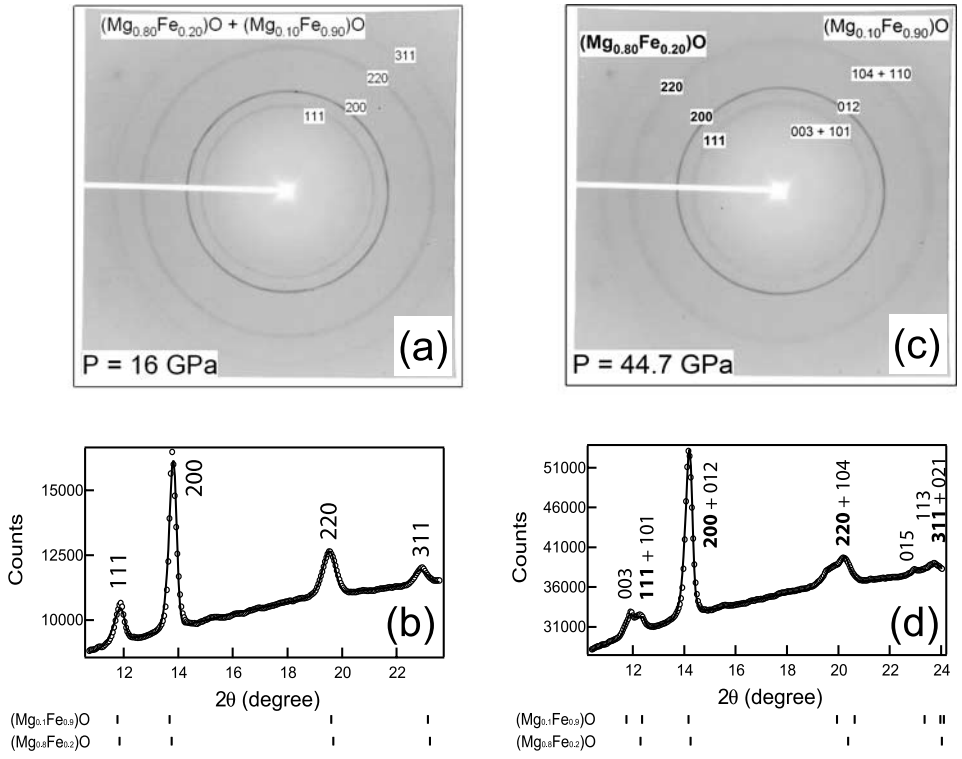

Figure 2. X-ray powder diffraction patterns of $(Mg_{0.8}Fe_{0.2})O$ + $(Mg_{0.1}Fe_{0.9})O$ (3:1 volume ratio), and integrated intensities vs. scattering angle (2θ) refined with the full-pattern fitting method: (a) Representative image and (b) integrated pattern before the structural transition of $(Mg_{0.1}Fe_{0.9})O$; (c) Representative image and (d) integrated pattern after the cubic to rhombohedral transition of $(Mg_{0.1}Fe_{0.9})O$.

composition undergoes a spin transition at pressures above 80 GPa [*Speziale et al.*, 2005], and therefore serves as a reference to document unit-cell volume (hence density) anomalies arising from the electronic transition of Fe^{2+} in $(Mg_{0.80}Fe_{0.20})O$. In particular, the (200) *d*-spacing, corresponding to half the cubic unit-cell parameter (*a*), can be tracked as a function of pressure: the difference in *d*-spacing for the two compositions, $\Delta d_{200} = d_{200}[(Mg_{0.10}Fe_{0.90})O] - d_{200}[(Mg_{0.80}Fe_{0.20})O]$, decreases continuously from 0.029 (±0.001) Å at ambient pressure to 0.012 (±0.002) Å at 40 GPa and then starts to increase again, reaching 0.027 (±0.001) Å by 62 GPa [*Speziale et al.*, 2005]. The reversal in the pressure dependence of Δd_{200} occurs at the same pressure, 40 GPa, at which Mössbauer spectroscopy indicates the onset of the HS to LS transition [*Speziale et al.*, 2005].

3.1. $(Mg_{0.10}Fe_{0.90})O$

[7] Above 20 GPa, we observe a structural transition from cubic (B1 structure type, space group $Fm\bar{3}m$) to rhombohedral (space group $R\bar{3}m$) (Figure 2), in good agreement with previous observations on Fe-rich magnesiowüstite [*Mao et al.*, 2002; *Lin et al.*, 2003; *Kondo et al.*, 2004]. As observed in previous experimental studies [*Mao et al.*, 2002; *Kondo et al.*, 2004] there is no resolvable discontinuity of molar volume across this structural transition, so we use the pressure dependence of the (012) d-spacing of the rhombohedral phase as a reference in the analysis of the pressure dependence of the (200) d-spacing of $(Mg_{0.80}Fe_{0.20})O$ (see above).

3.2. $(Mg_{0.80}Fe_{0.20})O$

[8] In line with previous results on similar compositions [*Jacobsen et al.*, 2005; *Lin et al.*, 2005], our data show that $(Mg_{0.80}Fe_{0.20})O$ remains cubic B1 structure to at least 62 GPa (Figure 2). Recent ambient-temperature experiments suggest that in the presence of non-hydrostatic stresses, $(Mg_{0.80}Fe_{0.20})O$ undergoes a slight rhombohedral distortion at pressures around 30 GPa [*Kantor et al.*, 2006b]. However, we did not observe this effect, perhaps because of better hydrostatic conditions in our experiments (e.g., due to annealing).

[9] A combined analysis of x-ray diffraction and Mössbauer data identifies the onset of the spin transition at 40 GPa at room temperature [*Speziale et al.*, 2005]. A Birch-Murnaghan equation of state (EoS) fit of the data below this pressure yields V_0 = 76.03 (±0.09) Å^3, K_{T0} = 158 (±3) GPa and K'_{T0} = 4.4 (±0.2), where $K'_{T0} = (\partial K_T/\partial P)_{T0}$. These values are in good agreement with independent static-compression measurements on Mg-rich magnesiowüstites, such as $(Mg_{0.64}Fe_{0.36})O$ (V_0 = 77.44 (±0.03) Å^3, K_{T0} = 154 (±3) GPa and K'_{T0} = 4.0 (±0.4); *van Westrenen et al.* [2005]) and $(Mg_{0.73}Fe_{0.27})O$ (V_0 = 77.30 ± 0.09 Å^3, K_{T0} = 153 (±3) GPa and K'_{T0} = 4.0 (±0.1); *Jacobsen et al.* [2005]). Our measurements are also in good agreement with those of *Lin et al.* [2005] for $(Mg_{0.83}Fe_{0.17})O$, even though their isotherm parameters differ significantly from ours because they fitted the data up to 56 GPa for the high-spin state and above ~75 GPa for the low-spin state. Despite the consistency of our bulk modulus value with values obtained from other static-compression measurements on Mg-rich magnesiowüstites, the zero-pressure unit-cell volumes are not so reproducible between studies (cf. the unit-cell volumes of $(Mg_{0.73}Fe_{0.27})O$ given by *Jacobsen et al.* [2002, 2005]). Elasticity measurements for Mg-rich magnesiowüstites suggest that, for compositions below 40 mol percent FeO, there is no resolvable variation in bulk modulus with composition at zero pressure: a variation of isothermal bulk modulus between 160 (±2) GPa for MgO and 154 (±3) GPa for $(Mg_{0.64}Fe_{0.36})O$ is given by x-ray diffraction measurements [*Fei*, 1999; *Dewaele et al.*, 2000; *van Westrenen et al.*, 2005], yet ultrasonic data show a variation of the isentropic bulk modulus between 160–162.5 (±3.0–0.5) GPa for pure MgO and 164–169 (±3–11) GPa for compositions between $(Mg_{0.63}Fe_{0.27})O$ and $(Mg_{0.6}Fe_{0.4})O$ [*Jackson et al.*, 1978; *Jackson and Niesler*, 1982; *Bonczar and Graham*, 1982; *Jacobsen et al.*, 2002].

[10] Our x-ray diffraction measurements on $(Mg_{0.8}Fe_{0.2})O$ are consistent with the data of *Lin et al.* [2005] for $(Mg_{0.83}Fe_{0.17})O$ up to the maximum common pressure of 62 GPa (Figure 3). Given this agreement, we combined the two data sets (Table 1) and fixed the starting volume to the value of 76.10 (±0.07) Å^3 reported by *Lin et al.* [2005]: identical within uncertainties with our measured starting volume, but more consistent with the systematics of V_0 versus composition of magnesiowüstites [*Jackson et al.*, 1978; *Jackson and Niesler*, 1982; *Bonczar and Graham*, 1982; *Jacobsen et al.*, 2002]. Our analysis does not include the results of *Jacobsen et al.* [2005] for $(Mg_{0.73}Fe_{0.27})O$ because the absolute ambient pressure volume for that composition (V_0 = 77.30 ± 0.02 Å^3) is not compatible (within mutual uncertainties) with either our values or the values obtained from systematics of V_0 versus composition [e.g., *Jacobsen et al.*, 2002].

[11] The Birch-Murnaghan EoS fit to the combined data set up to 40 GPa (high-spin phase) yields K_{T0} = 157.5 (±0.5) GPa and K'_{T0} = 3.92 (±0.1) (Figure 3), consistent with the most recent results for Mg-rich magnesiowüstites as discussed above. This value of K'_{T0} is lower than that obtained by fitting only the data for $(Mg_{0.80}Fe_{0.20})O$, and it is difficult to compare with other existing results for Mg-rich magnesiowüstites due to the substantial inconsistency between different techniques and even between different studies performed using the same techniques [e.g., *Jackson et al.*, 1978; *Bonczar and Graham*, 1982; *Richet et al.*, 1989; *Fei et al.*, 1992; *Jacobsen et al.*, 2002, 2005; *van Westrenen et al.*, 2005].

3.3. The Isothermal Equation of State of Low-Spin $(Mg_{0.80-0.83}Fe_{0.20-0.17})O$

[12] In order to determine the effect of the electronic spin-pairing transition on the density and elasticity of Mg-rich magnesowüstite, we need to know the equation of state for the low-spin phase. Studies to date on a range of similar (Mg-rich) magnesiowüstite compositions show that the transition is complete by pressures of 70 to 80 GPa (Figure 1) [*Badro et al.*, 2003; *Lin et al.*, 2005; *Speziale et al.*, 2005; *Lin et al.*, 2006a, 2007b; *Kantor et al.*, 2006a, 2007]. For this reason, we focus our analysis of the low-spin $(Mg_{1-x}Fe_x)O$ (x = 0.17–0.2) on the data of *Lin et al.*'s [2005] (Table 1) because these are the only x-ray diffraction measurements accessing the appropriate pressure range. Following the approach outlined by *Jeanloz* [1981], we calculate the Eulerian strain referred to the zero-pressure

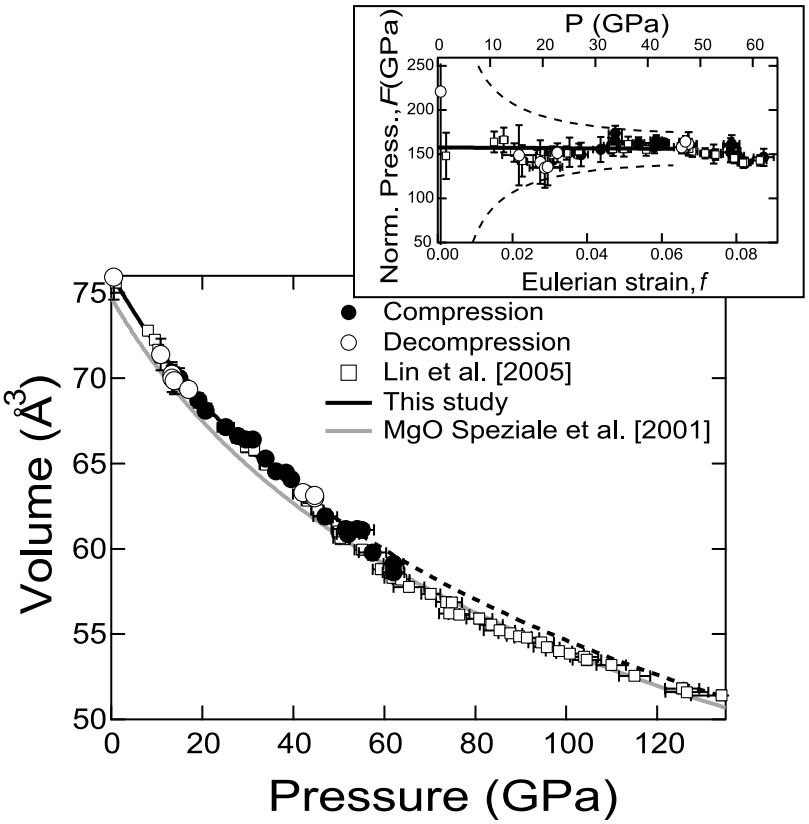

Figure 3. Isothermal compression curves of $(Mg_{1-x}Fe_x)O$ (x = 0.17–0.2), based on the combined data sets from the present study and from *Lin et al.* [2005]. The black curve is the 300 K isotherm for the high-spin state, as determined by fitting the data between 0 and 40 GPa with the Birch–Murnaghan equation (extrapolated to high pressure as a dashed line). The grey curve is the MgO isotherm after *Speziale et al.* [2001]. *Inset*: the same data shown as normalized pressure ($F = P/[3f(1 + 2f)^{5/2}]$) versus Eulerian strain ($f = 0.5[(V_0/V)^{2/3} - 1]$) yield the solid curve as the best fit isotherm for the high-spin phase, and the dashed curves represent 1σ uncertainties.

volume of the high-spin phase (V_0^{HS}), $g = 0.5[(V_0^{HS}/V)^{2/3} - 1]$, for both the high-spin and low-spin phases of $(Mg_{1-x}Fe_x)O$ (x = 0.17–0.2), and examine $G = F \cdot g$ versus g where F is the normalized pressure (see inset in Figure 3). This analysis reveals an anomalous change in slope at 40 GPa, and a region with reduced slope between 40 and 80 GPa followed by a region with higher slope above 80 GPa that we attribute to the low-spin phase (Figure 4). The changes in compression-behavior at 40 GPa and 80 GPa are clearly evident in the upper-left inset of Figure 4, where the residuals with respect to the model isotherm for the high-spin phase are plotted versus pressure.

[13] The compression of the low-spin phase of $(Mg_{1-x}Fe_x)O$ (x = 0.17–0.2) is similar to that of pure MgO (Figure 3): the unit-cell volumes agree to within 1 percent over the 80–135 GPa pressure range, in good accord with the findings of *Fei et al.* [2005]. In detail, however, the bulk modulus of low-spin $(Mg_{1-x}Fe_x)O$ (x = 0.17–0.2) appears to be ~13.9 (±0.1) percent higher than that of MgO as a function of pressure (lower-right inset in Figure 4). A second-order polynomial G versus g fit to Lin et al.'s low-spin data (equivalent to a third order Burch-Murnaghan equation of state) yields V_0 = 71 (±5) Å^3, K_{T0} = 186 (±150) GPa and $(\partial K_T/\partial P)_{T0}$ = 4.6 (±2.7). Evidently, the zero-pressure parameters are only weakly constrained due to the relatively small range of strain covered by the available data, along with the long extrapolation from 80 GPa to ambient pressure. Still, the best fit value of unit-cell volume at ambient conditions corresponds to a ratio V_0^{LS}/V_0^{HS} = 0.94 (±0.06), compatible with the value of 0.957 (±0.005) expected for $(Mg_{1-x}Fe_x)O$ (x = 0.17–0.2) based on the predicted ionic radius of low- versus high-spin Fe^{2+} in octahedral coordination in oxides [*Shannon and Prewitt*, 1969]. Our experimental results are also in agreement with the 0 K compression curves of the high- and low-spin phases of $(Mg_{0.8125}Fe_{0.1875})O$ calculated by *Tsuchiya et al.* [2006] (Figure 4). In addition, our estimated value of V_0^{LS}/V_0^{HS} = 0.94, based on experimental results, agrees with the value of 0.95 from the *ab initio* calculations of *Tsuchiya et al.* [2006].

[14] We have computed Eulerian strain f and normalized stress F for the low-spin phase of $(Mg_{1-x}Fe_x)O$ (x = 0.17–0.2) for thirteen values of zero pressure unit-cell volumes, between 66.97 and 76.10 Å^3 covering the 1σ uncertainty in the volume obtained from the G versus g analysis. For each case, we have performed a Birch-Murnaghan fit of the F versus f data. The trade-off between zero-pressure equation-of-state properties for the low-spin state is evident (Table 2). The goodness of fit, expressed by the χ^2 parameter, is insensitive to the assumed value for the zero-pressure volume of the low-spin state ranging between

Table 1. Unit Cell Volume of $(Mg_{0.8}Fe_{0.2})O$ and $(Mg_{0.83}Fe_{0.17})O$ at High Pressure

$(Mg_{0.8}Fe_{0.2})O$			$(Mg_{0.83}Fe_{0.17})O$[a]		
Pressure, GPa	V, Å^3	Experimental Details	Pressure, GPa	V, Å^3	Experimental Details
10^{-4}	76.30 ± 0.25		10^{-4}	76.10 ± 0.07	
.5 ± 0.2	75.93 ± 0.95	Decomp.	1.0 ± 0.1	75.60 ± 0.02	Comp.
10.8 ± 0.1	71.39 ± 0.92	Decomp.	8.0 ± 0.5	72.78 ± 0.08	Comp.
13.0 ± 1	70.24 ± 0.70	Decomp.	9.6 ± 0.5	72.25 ± 0.22	Comp.
13.3 ± 0.7	70.00 ± 0.80	Decomp.	10.3 ± 0.6	71.66 ± 0.12	Comp.
13.8 ± 0.4	69.85 ± 0.78	Comp.	10.8 ± 1.2	71.22 ± 0.23	Comp.
15.0 ± 2	70.00 ± 0.59	Comp.	13.2 ± 0.7	70.42 ± 0.17	Comp.
17.0 ± 0.5	69.34 ± 0.35	Decomp.	14.4 ± 1.2	69.95 ± 0.23	Comp.
19.0 ± 2	68.70 ± 0.43	Comp.	16.0 ± 0.8	69.58 ± 0.22	Comp.
21.0 ± 1	68.11 ± 0.35	Comp.	18.5 ± 0.4	68.86 ± 0.25	Comp.
25.0 ± 2	67.12 ± 0.37	Comp.	20.9 ± 0.6	68.23 ± 0.28	Comp.
27.8 ± 0.5	66.61 ± 0.36	Comp.	27.5 ± 0.8	66.53 ± 0.29	Comp.
30.0 ± 1	66.41 ± 0.32	Comp.	29.6 ± 0.9	66.00 ± 0.34	Comp.
31.1 ± 0.6	66.41 ± 0.30	Comp.	31.4 ± 0.9	65.79 ± 0.33	Comp.
33.9 ± 0.6	65.29 ± 0.27	Comp.	33.9 ± 1.4	64.94 ± 0.15	Comp.
36.0 ± 1	64.55 ± 0.27	Comp.	43.1 ± 1.3	62.83 ± 0.23	Comp.
38.4 ± 0.5	64.46 ± 0.27	Comp.	43.4 ± 1.3	62.96 ± 0.15	Comp.
39.5 ± 0.1	64.08 ± 0.21	Comp.	45.3 ± 1.4	62.26 ± 0.21	Comp.
42.1 ± 0.4	63.30 ± 0.34	Decomp.	47.2 ± 1.4	61.81 ± 0.23	Comp.
43.0 ± 3	63.20 ± 0.27	Comp.	50.1 ± 1.5	61.01 ± 0.23	Comp.
44.7 ± 0.9	62.99 ± 0.36	Decomp.	50.3 ± 1.5	60.63 ± 0.23	Comp.
44.7 ± 0.8	63.13 ± 0.27	Decomp.	50.9 ± 1.5	60.55 ± 0.23	Comp.
47.0 ± 3	61.89 ± 0.41	Comp.	55.1 ± 1.7	59.94 ± 0.28	Comp.
52.0 ± 3	61.16 ± 0.41	Comp.	59.2 ± 1.8	58.80 ± 0.27	Comp.
52.0 ± 3	60.85 ± 0.26	Comp.	61.8 ± 1.9	58.29 ± 0.27	Comp.
54.0 ± 2	61.15 ± 0.31	Comp.	63.7 ± 1.9	58.20 ± 0.27	Comp.
55.0 ± 3	61.12 ± 0.33	Comp.	65.4 ± 3.4	57.76 ± 0.27	Comp.
57.0 ± 3	59.78 ± 0.41	Comp.	70.2 ± 2.1	57.35 ± 0.27	Comp.
62.0 ± 2	58.61 ± 0.36	Comp.	73.6 ± 2.2	56.87 ± 0.22	Comp.
62.0 ± 2	59.13 ± 0.31	Comp.	74.3 ± 2.2	56.20 ± 0.24	Comp.
			74.8 ± 2.2	56.85 ± 0.24	Comp.
			76.4 ± 2.3	56.15 ± 0.26	Comp.
			80.9 ± 2.8	55.89 ± 0.29	Comp.
			83.5 ± 2.5	55.55 ± 0.24	Comp.
			85.3 ± 3.4	55.22 ± 0.22	Comp.
			87.7 ± 2.6	55.04 ± 0.22	Comp.
			89.6 ± 2.7	54.87 ± 0.26	Comp.
			91.3 ± 2.7	54.78 ± 0.24	Comp.
			94.5 ± 2.8	54.50 ± 0.26	Comp.
			95.7 ± 2.9	54.24 ± 0.26	Comp.
			98.4 ± 3	54.01 ± 0.24	Comp.
			100.8 ± 3	53.86 ± 0.21	Comp.
			103.9 ± 3.1	53.66 ± 0.23	Comp.
			104.5 ± 3.1	53.49 ± 0.30	Comp.
			109.9 ± 3.3	53.18 ± 0.27	Comp.
			115.0 ± 3.5	52.55 ± 0.21	Comp.
			125.4 ± 3.8	51.80 ± 0.29	Comp.
			126.5 ± 4.7	51.59 ± 0.20	Comp.
			134.1 ± 6.7	51.41 ± 0.29	Comp.

[a]Experimental details are reported in *Lin et al.* [2005]. Comp. measurement performed in compression. Decomp. measurements performed on decompression.

V_0^{LS} = 66.97 and 76.10 Å^3 (equivalent to V_0^{LS}/V_0^{HS} between 0.88 and 1.0). That is, the model equation of state's misfit in pressure over this range of V_0^{LS} is 1.3–1.5 GPa, which is less than half the average uncertainty in the experimental pressures, and there is a large trade-off with model norm expressed as χ^2 (Table 2). However, we can reduce the range of reasonable V_0^{LS}/V_0^{HS} ratios to 0.91–0.97 based on considerations of K_{T0}. V_0^{LS}/V_0^{HS} ratios lower than 0.91 and higher than 0.97 correspond to values of fitted K_{T0}^{LS} which are more than 40 percent higher and 20 percent lower, respectively, than K_{T0}^{HS}. Assuming that the difference in $K_{T0}^{LS} - K_{T0}^{HS}$ of $(Mg_{0.80-0.83}Fe_{0.20-0.17})O$ is equal to that of the FeO component weighted by its molar fraction, we would have a factor of two increase in K_{T0} of the FeO component in the case $V_0^{LS}/V_0^{HS} < 0.91$ and a factor of one decrease of K_{T0} for the case $V_0^{LS}/V_0^{HS} > 0.97$. We thus consider V_0^{LS}/V_0^{HS} ratios only in the range of 0.91–0.97; this allows us to constrain K_{T0} to 246–136 GPa and $(\partial K_T/\partial P)_{T0}$ to 3.6–5.4 for the low-spin phase of $(Mg_{0.83-0.8}Fe_{0.17-0.2})O$.

3.4. Modeling the Effects of a Sharp Transition

[15] To put the trade-off associated with uncertainties in the zero-pressure properties of the low-spin equation of state into perspective, we consider the differences in volume, bulk modulus and bulk sound velocity ($v_\phi = (K_S/\rho)^{1/2}$ where ρ is density) across the spin transition as a function of pressure across the lower mantle for all the models between

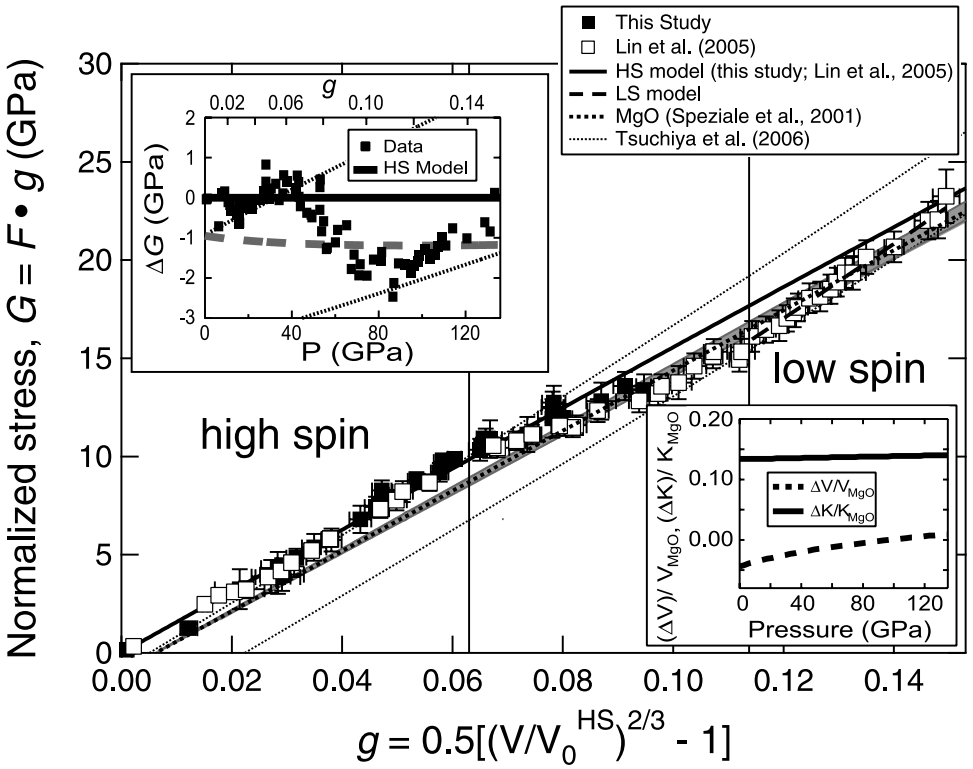

Figure 4. Static-compression results for $(Mg_{1-x}Fe_x)O$ (x = 0.17–0.2) plotted in terms of normalized pressure G versus Eulerian strain referred to the starting volume of the high-spin phase, g (see text). Data between 40 and 80 GPa are interpreted as coexisting high-spin and low-spin phases, whereas data above 80 GPa are assigned to the low-spin state. The solid black line is the isotherm for the high-spin phase determined by fitting the data below 40 GPa with the Birch–Murnaghan equation of state. The dashed line is the isotherm for the low-spin phase, and the dotted curve is the MgO isotherm of *Speziale et al.* [2001] with the grey area indicating its 1σ uncertainty. The thin dotted lines are the 0 K compression curves of the high- and low-spin $(Mg_{0.875}Fe_{0.125})O$ by *Tsuchiya et al.* [2006]. The inset at the top left shows the deviation of the experimental data from the isotherm for the high-spin phase (solid squares), with the dashed grey line giving the deviation of the MgO isotherm, and the dotted lines giving the deviation of the first principles high- and low-spin isotherms by *Tsuchiya et al.* [2006]. The inset at the bottom right shows the relative difference of unit-cell volume $(V - V_{MgO})/V_{MgO}$ and bulk modulus $(K - K_{MgO})/K_{MgO}$ between the low-spin phase of $(Mg_{1-x}Fe_x)O$ (x = 0.17–0.2) and pure MgO.

V_0^{LS}/V_{0s}^{HS} = 0.91 and 0.97 (Figure 5). In our analysis, we use results obtained at ambient temperature, and assume that the difference in bulk sound velocity between the two phases is unaffected by the conversion from isothermal to adiabatic modulus. In addition, we only consider the change in properties between high- and low-spin "end-member" phases, without considering that the coexistence of the high-spin and low-spin state of Fe^{2+} may result in partitioning of HS and LS intermediate compositions in the MgO – FeO system [*Dubrovinsky et al.*, 2000], which still have to be thoroughly explored both experimentally and theoretically [*Lin et al.*, 2003; *Kondo et al.*, 2004; *Tsuchiya et al.*, 2006].

[16] Over the range of models of the low-spin phase (expressed by the zero-pressure volumes considered here, V_0^{LS}/V_0^{HS} = 0.91 to 0.97), the volume decrease ranges from 3.7 (±0.5) percent if the transition takes place at 40 GPa to 2.0 (±0.1) percent if it takes place at 80 GPa. The effect of pressure is greater, over this range, than the uncertainty in the zero-pressure volume of the low-spin phase. Similarly, uncertainty in the zero-pressure volume becomes less important as one considers the jump in bulk modulus or bulk sound velocity with increasing pressure: $\Delta K_T/K_T^{HS} \approx$

Table 2. Fit Parameters of the 3rd Order Birch–Murnaghan Isotherm of the Low-Spin Phase of $(Mg_{0.8}Fe_{0.2})O$ for Various Initial Ratios V_0^{LS}/V_0^{HS}

V_0^{LS}/V_0^{HS}	K_0, GPa	K_0'	χ^2	RMS misfit, GPa
0.88	339 ± 28	3.0 ± 0.7	0.782	1.55
0.89	304 ± 27	3.3 ± 0.7	0.780	1.49
0.90	273 ± 26	3.6 ± 0.7	0.784	1.45
0.91	246 ± 25	3.9 ± 0.7	0.793	1.41
0.92	222 ± 24	4.1 ± 0.8	0.804	1.39
0.93	200 ± 23	4.4 ± 0.8	0.817	1.37
0.94	182 ± 22	4.7 ± 0.8	0.831	1.36
0.95	165 ± 22	4.9 ± 0.8	0.845	1.35
0.96	149 ± 21	5.2 ± 0.8	0.858	1.34
0.97	136 ± 20	5.4 ± 0.9	0.872	1.34
0.98	123 ± 20	5.7 ± 0.9	0.884	1.33
0.99	112 ± 19	6.0 ± 0.9	0.897	1.33
1.00	101 ± 19	6.2 ± 0.9	0.908	1.32

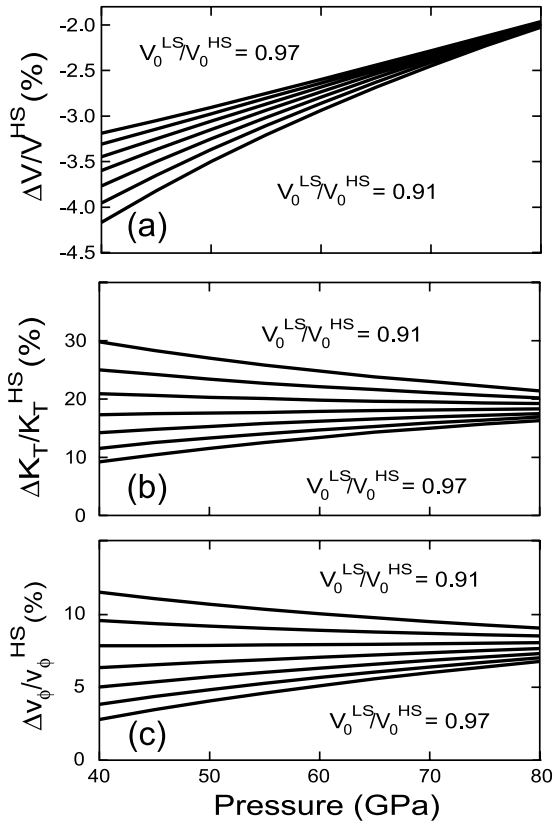

Figure 5. Calculated percentage differences in unit-cell volume (a), bulk modulus (b) and bulk sound velocity (c) between the the high- and low-spin forms of $(Mg_{1-x}Fe_x)O$ (x = 0.17–0.2) at pressures between 40 and 80 GPa. The different curves show results for starting-volume ratios V_0^{LS}/V_0^{HS} ranging between 0.91 and 0.97 at fixed intervals of 0.01 V_0^{LS}/V_0^{HS}.

20 (±10–3) percent and $\Delta v_\phi/v_\phi^{HS} \approx 7.6$ (±4–1.2) percent over the pressure range 40–80 GPa. If we assume the value $V_0^{LS}/V_0^{HS} = 0.957$, as indicated by ionic-radius systematics [*Shannon and Prewitt*, 1969], we find that $\Delta V/V^{HS}$, $\Delta K_T/K_T^{HS}$ and $\Delta v_\phi/v_\phi^{HS}$ vary from −3.3 to −2.0 percent, 12 to 17 percent and 3.8 to 7.0 percent, respectively, at pressures of 40–80 GPa (Figure 5). If we assume that high temperature has little effect upon the sharpness of the transition, these results provide bounds for the overall volume (or density) and velocity change resulting from the spin transition of Fe^{2+} in magnesiowüstite at lower-mantle conditions, based on the available experimental results [*Speziale et al.*, 2005; *Lin et al.*, 2005; *Kantor et al.*, 2005; *Fei et al.*, 2005; *Lin et al.*, 2006b; *Lin et al.*, 2007a, 2007b]. However, these effects would be reduced, if the spin transition would turn into a spin crossover with an extended transition pressure under lower-mantle conditions as indicated theoretically [*Sturhahn et al.*, 2005; *Tsuchiya et al.*, 2006].

[17] As the abundance of magnesiowüstite is expected to be only of the order of 30 percent in the lower mantle based on a pyrolite model, we have to scale the effects of the spin transition in a consistent manner in order to assess seismologically observable effects. To derive conservative estimates of the influence of the Fe-spin transition on the properties of the lower mantle, we neglect the possibility of a high- to low-spin transition in Mg-Fe silicate perovskite (which, due to its more complex structure may be less sensitive to variations in Fe^{2+} ionic size) and predicted temperature effects on the spin transition in magnesiowüstite [*Sturhahn et al.*, 2005; *Tsuchiya et al.*, 2006]. We thus estimate that the overall effect of the transition is 0.6 (±0.1)–1.1 (±0.2) percent density increase, and 2.4 (±0.5)–2.3 (±1.0) percent bulk sound velocity increase as the transition pressure is varied between 40 and 80 GPa. These changes are comparable to the major discontinuities of the upper mantle and transition zone ($\Delta v_\phi \sim 2$–3.2 and ~3.4–5.5 percent at the 410 and 660 km for *Dziewonski and Anderson*'s [1981] PREM and for *Kennett et al.*'s [1995] ak135, respectively), and would cause visible seismic anomalies if the spin transition takes place over a narrow depth range.

3.5. Modeling the Effects of a Continuous Transition Across a Large Pressure Range

[18] Various thermodynamic arguments suggest that the effect of temperature is (a) to increase the spin-transition pressure by 0.015–0.018 GPa/K [*Sherman*, 1988; *Badro et al.*, 2005; *Lin et al.*, 2005] up to 0.04 GPa/K [*Hofmeister*, 2006] for magnesiowüstites with compositions relevant for the lower mantle; and (b) to broaden the pressure range of the transition to several tens of GPa along the mantle geotherm [*Sturhahn et al.*, 2005; *Tsuchiya et al.*, 2006]. However, experiments do not show clear evidence for these temperature effects [*Badro et al.*, 2003; *Lin et al.*, 2005; *Speziale et al.*, 2005; *Fei et al.*, 2005; *Kantor et al.*, 2006a; *Kantor et al.*, 2007], or they even suggest a negative temperature dependence of the spin crossover pressure [*Kantor et al.*, 2005]. In order to assess the effects of the spin transition broadening, we have analyzed two scenarios for the HS to LS transition. In the first, the transition is considered independent of temperature and it takes place between 40 and 80 GPa (the pressure range observed in our Mössbauer and x-ray diffraction experiments). In the other scenario, the transition is modeled between 30 and 120 GPa, corresponding to the transition range predicted by *Sturhahn et al.* [2005] based on a mean-field (Bragg-Williams) model for order-disorder transformations in alloys [*Williams*, 1935], and by *Tsuchiya et al.* [2006] based on LDA + U with internally consistent static-lattice energy calculations supplemented by thermodynamic arguments to describe the temperature-induced increase of the low-spin Fe^{2+} population in diluted $(Mg_{1-x}Fe_x)O$ solid-solutions (Figure 6).

3.6. Transition Between 40 and 80 GPa

[19] In order to calculate the effect of a progressive transformation, we assume that the properties of Mg-rich magnesiowüstite across the transition are averages of those of the low-pressure and of the high-pressure phases weighted by their relative molar fractions as determined by high-pressure Mössbauer spectroscopy, and assuming that the pressure range at which the transition takes place is not temperature dependent [*Speziale et al.*, 2005]. This last assumption is justified by the agreement between the transition pressure ranges determined at T = 10 K on $(Mg_{0.80}Fe_{0.20})O$ (40–80 GPa; *Speziale et al.* [2005]), at 300 K on $(Mg_{0.83}Fe_{0.17})O$ (49–75 GPa; *Badro et al.*,

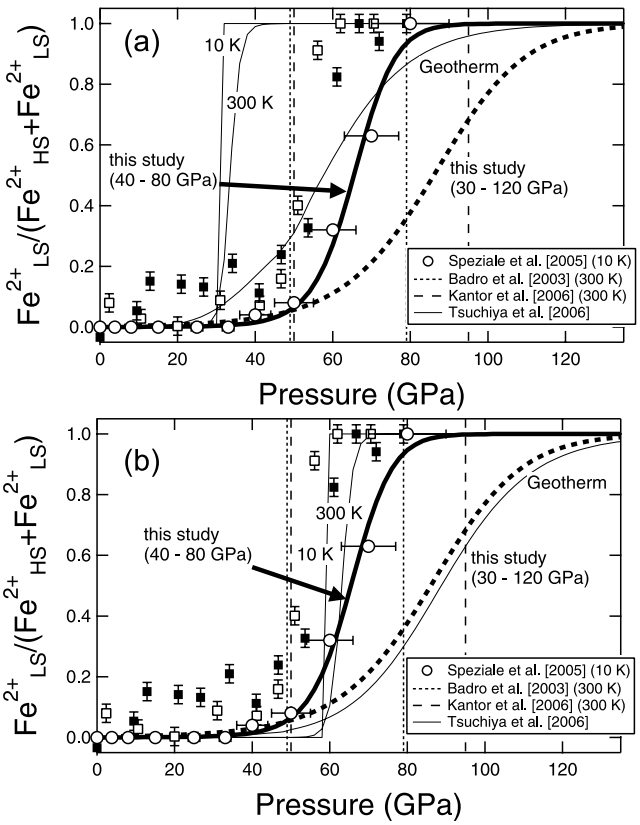

Figure 6. (a) Models of the pressure dependence of the abundance of low-spin relative to high-spin states, compared with experimental results obtained by Mössbauer spectroscopy [*Speziale et al.*, 2005]. The thick solid and dashed curves indicate the models for a progressive transition between 40 and 80 GPa and between 30 and 120 GPa, respectively. The thin lines represent the pressure dependence of the low-spin fraction at 10 K, 300 K, and along a mantle geotherm after *Tsuchiya et al.* [2006]. The vertical dotted and dashed lines are the experimental pressure ranges for the spin transition based on the results of *Badro et al.* [2003] and *Kantor et al.* [2006a]. (b) Our model compared with the model by *Tsuchiya et al.* [2006] modified to have agreement with the experimental transition pressure (see text). The small filled and open squares are the results of X-ray emission spectroscopy of $(Mg_{0.75}Fe_{0.25})O$ and $(Mg_{0.95}Fe_{0.05})O$ by *Lin et al.* [2005] and *Lin et al.* [2007b] respectively.

2003]), and more recently on $(Mg_{0.80}Fe_{0.20})O$ at 300 K (50–<100 GPa; [*Kantor et al.*, 2006a; *Kantor et al.*, 2007]). However, it is true that the thermal energy at 10 K–300 K is much less significant than at high T above 2000 K, and these experiments are not inconsistent with the hypothesis of a substantial temperature dependence of the transition pressure. More high temperature experimental studies are needed to clarify this point.

[20] We calculate the pressure dependence of the fraction of low-spin phase by using the empirical equation

$$^{LS}Fe/\left(^{HS}Fe + {}^{LS}Fe\right) = 1/\left[1 + A\exp\left(B + CX_P + 0.5\ D\ X_P^2\right)\right], \quad (1)$$

where ^{LS}Fe and ^{HS}Fe represent the molar fractions ($^{LS}Fe + {}^{HS}Fe = 1$) of the two phases of $(Mg_{1-x}Fe_x)O$ ($x = 0.17–0.2$), and $X_P = (P - P_i)/(P_f - P_i)$, where P_i and P_f are the pressures at which the transition begins and is completed based on experimental results. The parameters A, B and D are determined by least squares fit to the low-spin Fe^{2+} abundance obtained by Mössbauer spectroscopy [*Speziale et al.*, 2005]. The best fit coefficients are A = 15 (±5), B = 1.5 (±0.9), C = −11.2 (±0.6), D = −2.7 (±0.3). The calculated pressure dependence of the low-spin fraction is plotted in Figure 6 in comparison with the experimental results of *Speziale et al.* [2005].

[21] We have calculated the relative change in unit-cell volume and bulk sound velocity during the progressive spin transition, $100 \cdot x\Delta V/V^{HS}$ and $100 \cdot x\Delta v_\phi/v_\phi^{HS}$ respectively, analyzed across the range of starting unit-cell volume ratio $0.91 < V_0^{LS}/V_0^{HS} < 0.97$ (here x is the molar fraction of the low-spin phase of Mg-rich magnesiowüstite, and $\Delta V/V^{HS}$ and $\Delta v_\phi/v_\phi^{HS}$ are calculated for the sharp transition as explained above). The average percent differences in unit-cell volume and bulk sound velocity, that is, the integral over the whole transition range (40–80 GPa) of the relative changes, is plotted in Figure 7. In the case of a transition

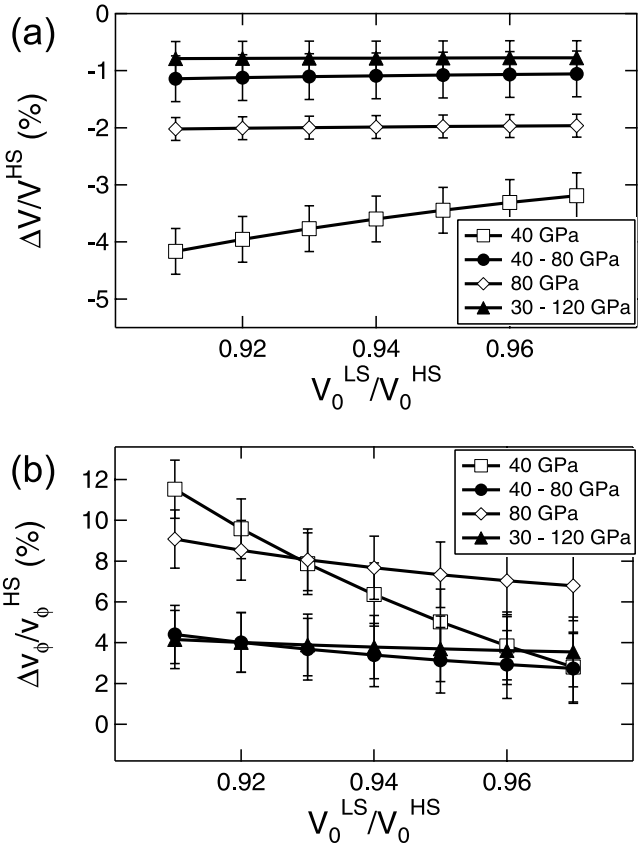

Figure 7. Summary of (a) the modeled unit-cell volume decrease and (b) bulk sound velocity increase for the cases of complete high- to low-spin transition at 40 GPa (open squares) and at 80 GPa (open circles), and for the cases of progressive transition between 40 and 80 GPa (filled circles) and between 30 and 120 GPa (filled triangles). The results are plotted as a function of assumed zero-pressure volume for the low-spin phase, with $V_0^{LS}/V_0^{HS} = 0.94$ being our preferred model.

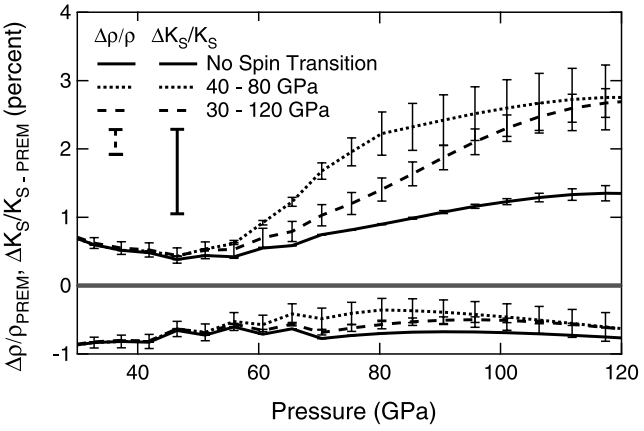

Figure 8. Relative density and bulk modulus variation between a pyrolitic mineralogical model and the PREM seismological model (see text for details). The three sets of curves represent: model with no spin transition in magnesiowüstite, a model with progressive spin transition across the pressure range 40–80 GPa and a model with spin transition across the range between 30 and 120 GPa. The large error bars under the legend correspond to 1σ when considering only the uncertainties in the thermal parameters θ_0, γ_0 and q for the three mineral phases in the models. The error bars along the curves reflect the uncertainties in the 300 K isotherms of the mineral phases of the models, so show how well resolved the systematic effects of the spin transition may be (assuming no compensating effects due to changes in thermal properties across the spin transition).

across the pressure range 40–80 GPa, the average volume decrease $\langle \Delta V/V^{HS} \rangle$ is 1.1 (±0.2) percent, and is insensitive to the assumed starting volume ratio V_0^{LS}/V_0^{HS} (Figure 7a), whereas the average velocity increase $\langle \Delta v_\phi/v_\phi^{HS} \rangle$ ranges from 4.4 (±1.6) percent at V_0^{LS}/V_0^{HS} = 0.91 to 2.7 (±1.6) percent at V_0^{LS}/V_0^{HS} = 0.97 (Figure 7b). For a model lower-mantle assemblage containing 30 mol percent Mg-rich magnesiowüstite, the average change in bulk sound velocity is 0.9–1.5 (±0.5) percent in case of the transition between 40 and 80 GPa. These predicted changes should be observable by seismology.

3.7. Transition Between 30 and 120 GPa

[22] In order to model the transition across a broader pressure range extended throughout the whole lower mantle, similar to the predictions by *Tsuchiya et al.* [2006] and *Sturhahn et al.* [2005] we have applied Equation (1) rescaled to the range 30–120 GPa (by changing the parameters P_i and P_f in Equation 1) by using the same best fit coefficients reported in the previous section (Figure 6a). The model pressure dependence of the low-spin fraction is very different from that calculated based on the results by *Tsuchiya et al.* [2006] along an adiabatic lower mantle thermal profile [*Brown and Shankland*, 1981] (Figure 6a). However, the discrepancy between our empirical model of the pressure dependence of the fraction of low-spin phase and the results of the computational study by *Tsuchiya et al.* [2006] is strongly reduced if we shift the transition pressure, determined by static-lattice total-energy calculations, from the value of 32 (±2) GPa to match the average central pressure of 65 (±7) GPa of the ranges determined by the experiments (Figure 6b). In particular, the model calculated along a geothermal P – T path is very similar to our empirical model for a broad transition between 30 and 120 GPa (Figure 6b).

[23] We have calculated, as in the previous scenario (transition between 40 and 80 GPa), the average relative changes in unit-cell volume and bulk sound velocity when we consider a broad transition between 30 and 120 GPa. Both the average changes in volume $\langle \Delta V/V^{HS} \rangle$ and bulk sound velocity $\langle \Delta v_\phi/v_\phi^{HS} \rangle$ are only slightly dependent on the starting volume ratio V_0^{LS}/V_0^{HS}, averaging 0.8 (±0.2) percent and 3.9 (±1.5) percent, respectively (Figure 7). For a model lower-mantle assemblage containing 30 mol percent Mg-rich magnesiowüstite, the average change in bulk sound velocity is 1.3 (±0.5) percent for a transition between 30 and 120 GPa. These changes are probably smaller than can be currently resolved by deep-mantle global seismology.

3.8. Fe Spin Transition in Magnesiowüstite: Implications for Lower-Mantle Mineralogical Models

[24] Even though a progressive transition would likely not produce a detectable seismic discontinuity, the corresponding changes in elastic properties of Mg-rich magnesiowüstite would affect the bulk-sound velocity of a typical lower-mantle mineral assemblage. The differences in

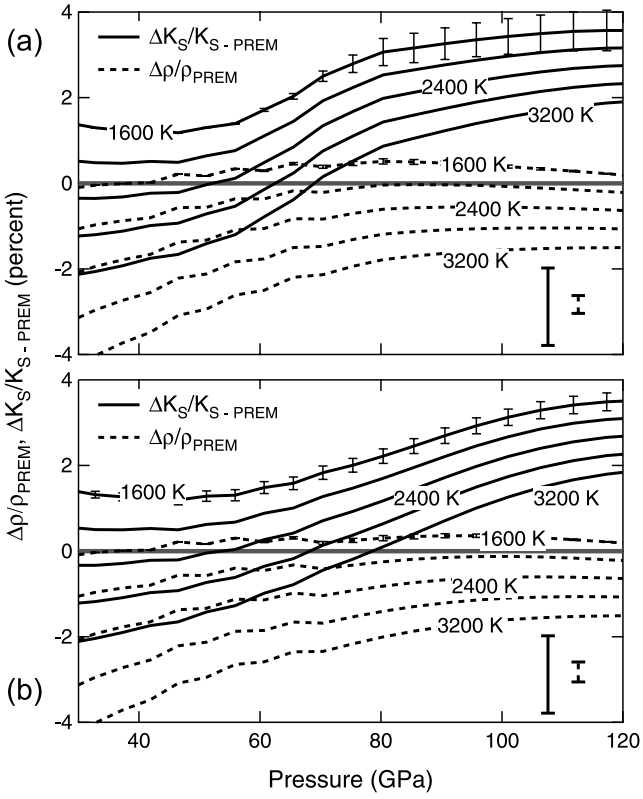

Figure 9. Relative density and bulk modulus variation between a pyrolitic mineralogical model and the PREM seismological model, shown as a function of temperature and including the effect of spin transition of Fe^{2+} in magnesiowüstite (see text for details). Cases are shown for a progressive spin transition across the pressure range 40–80 GPa (a) and 30–120 GPa (b), with error bars as in Figure 8.

Table 3. Parameters of the 3rd Order Birch–Murnaghan Equation of State and Debye Model for $(Mg_{0.89}Fe_{0.11})SiO_3$, the Low-Spin and High-Spin Phases of $(Mg_{0.83}Fe_{0.17})O$[a]

Par.	$(Mg_{0.88}Fe_{0.06}Al_{0.12}Si_{0.94})O_3$	$(Mg_{0.83}Fe_{0.17})O$ (HS)	$(Mg_{0.83}Fe_{0.17})O$ (LS)	$CaSiO_3$
V_0, Å^3	163.9[b]	76.10[e]	71.39[e]	45.37 ± 0.1[f]
Mol. wt., g	102.38	45.67	45.67	116.17
ρ_0, g/cm^3	4.016[b]	3.859[b]	3.859[b]	4.12 ± 0.1[f]
K_{T0}, GPa	260 ± 10[c]	157.5 ± 0.5[e]	186 ± 22[e]	259 ± 20[f]
$(\partial K_T/\partial P)_{T0}$	4.03 ± 0.03[d]	3.92 ± 0.1[e]	4.6 ± 0.8[e]	3.9 ± 0.1[f]
θ_0, K	1009 ± 9[b]	587 ± 80[b]	587 ± 80[b]	1100[b]
γ_0	1.64 ± 0.3[b]	1.46 ± 0.05[b]	1.46 ± 0.05[b]	1.7[b]
q	1.75 ± 0.7[b]	1.2 ± 0.1[b]	1.2 ± 0.1[b]	1[b]

[a]The uncertainties reported in this table are estimated ranges of variation between the available literature data.
[b]*Lee et al.* [2004] – average of high- and low-thermal expansion set of parameters (see *Lee et al.* [2004] for details).
[c]Average of *Lee et al.* [2004] and *Jackson et al.* [2004].
[d]Average of *Lee et al.* [2004] and *Vanpeteghem et al.* [2006].
[e]This study.
[f]Average of *Shim et al.* [2000] and *Lee et al.* [2004].

bulk elastic properties between a pyrolite-like mineralogical model with and without the effects of the spin transition could be misinterpreted as being due to changes in bulk composition or temperature at depth. In order to explore these effects, we considered a mineral assemblage consisting of a ternary mixture of 64 mol percent $(Mg_{0.88}Fe_{0.06}Al_{0.12}Si_{0.94})O_3$ perovskite, 31 mol percent $(Mg_{1-x}Fe_x)O$ (x = 0.17–0.2) and 5 mol percent $CaSiO_3$, which is close to an undepleted natural peridotite [*Lee et al.*, 2004]. We compared the density and bulk sound velocity of this assemblage, assuming either 1) a progressive spin transition across two different pressure ranges (40–80 GPa and 30–120 GPa) or 2) no transition, and evaluated results along selected isotherms as well as along a pressure-temperature path corresponding to estimated lower-mantle geotherms (Figures 8 and 9) [*Dziewonski and Anderson*, 1981; *Brown and Shankland*, 1981].

[25] Our calculations follow the basic principles of several studies of the mineralogical composition of the lower mantle, both based on experimental thermoelastic parameters of the mineral components [e.g., *Weidner*, 1994; *Jackson*, 1998; *Mattern et al.*, 2005] or based on ab initio computations [e.g., *Marton and Cohen*, 2002; *Wentzcovitch et al.*, 2004] and tested in comparison with average physical properties (seismic velocity and density) of a reference seismological Earth model such as PREM [*Dziewonski and Anderson*, 1981]. The new aspect included in our model is the effect of the Fe^{2+} spin transition in magnesiowüstite based on experimental results, unavailable until now.

[26] We performed the calculations assuming V_0^{LS}/V_0^{HS} = 0.94, corresponding to our preferred model for Mg-rich magnesiowüstite. The density and bulk modulus for the different phases were calculated using the Birch-Murnaghan formalism and the Debye model for the thermal pressure [e.g., *Jackson and Rigden*, 1996]. The Debye temperature (θ_0), Grüneisen parameter (γ_0) and its logarithmic volume derivative (q) for the three minerals were obtained as averages of the two sets used by *Lee et al.* [2004] (see discussion in *Lee et al.* [2004]). The bulk modulus and pressure derivative of (Mg, Fe)(Al, Si)O_3 perovskite were averages of those presented by *Lee et al.* [2004] and those from *Jackson et al.* [2004] and *Vanpeteghem et al.* [2006], respectively (Table 3). The unit-cell volume and the bulk modulus and pressure derivative for $CaSiO_3$ perovskite were averages of those used by *Lee et al.* [2004] and those by *Shim et al.* [2000], and the bulk modulus and pressure derivative for magnesiowüstite were those determined in the present study. In our calculations, we neglected the effect of any spin transition on the elastic properties of Mg-silicate perovskite due to the absence of relevant experimental data (this also means that our results are conservative, in that spin effects in the perovskite are likely to enhance the effects we calculate here). The pressure dependence of the molar fraction of low-spin Mg-rich magnesiowüstite is the same used in the above calculations. Finally, we limited our calculations to the lower mantle above the D″ region, and did not consider the effects of the transition from Mg-perovskite to post-perovskite phases [*Murakami et al.*, 2004; *Shim et al.*, 2004; *Oganov and Ono*, 2004]. All the parameters used for our calculations are summarized in Table 3.

[27] Assuming that high temperature does not modify the relative change in volume and bulk modulus across the spin transition, we observe that along the pressure-temperature path corresponding to the geotherm calculated by *Brown and Shankland* [1981] the occurrence of the spin transition in magnesiowüstite causes a difference of bulk modulus $\Delta K_S/K_{S\text{-PREM}} = (K_{S\text{-Model}} - K_{S\text{-PREM}})/K_{S\text{-PREM}}$ between a pyrolite-type mineral assemblage and the PREM reference model of up to 2.8 percent at the maximum pressure of 120 GPa, approximately 2 times larger than is the case in the absence of the spin transition (Figure 8). The effect of the spin transition on density is less significant: $\Delta\rho/\rho_{\text{-PREM}} = -0.66$, 15 percent smaller than in the case of no spin transition. The difference between models that do and do not include the spin transition are significant relative to the uncertainties in the elastic moduli and volumes. Uncertainties in the thermal parameters (γ_0, θ_0, q) apply to all the models, so should not affect our conclusions about the significance of the spin transition (Figure 8).

[28] Based on the available data, we can only provide tentative estimates of the effects of temperature, mineralogical composition and degree of completion of the spin transition on the density and bulk modulus of model lower-mantle assemblages. The effect of temperature is to decrease the bulk modulus of the assemblage, approaching

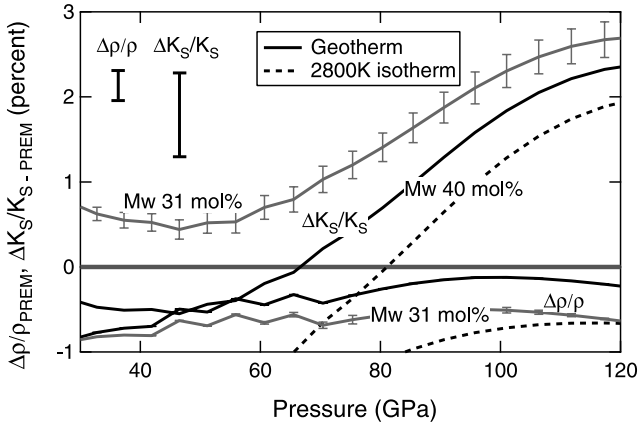

Figure 10. Relative density and bulk modulus variation with respect to PREM of a pyrolite-like mineralogical model with progressive spin transition in magnesiowüstite between 30 and 120 GPa. The effect of increasing the amount of magnesiowüstite from 31 to 40 mol percent, both along a geotherm and along a 2800 K isotherm, is shown, along with a model with 31 mol percent magnesiowüstite (standard pyrolite of *Lee et al.* [2004]) along a geotherm *P-T* path.

the PREM model, but also to decrease the overall density, below that of the reference Earth model (Figure 9). Increasing the amount of Mg-rich magnesiowüstite has the advantage of increasing the overall density at the highest pressures, but also of decreasing the bulk modulus (Figure 10). Finally, as suggested by *Sturhahn et al.* [2005] and *Tsuchiya et al.* [2006], a substantial temperature dependence of the spin-transition pressure and broadening of the spin transition (even beyond the pressure range of the lower mantle) would mitigate the very large rise of the bulk modulus of magnesiowüstite of a model mantle assemblage with respect to the reference PREM model (Figure 8). Thus with the simplifying assumption that the thermal parameters of the equation of state of Mg-rich magnesiowüstite are not affected by the spin-transition, we expect that the lowermost part of the lower mantle is either characterized by a very high thermal gradient (more than 80 percent larger than that predicted by *Brown and Shankland* [1981]) or by depletion of the SiO_2 content (to less than 55 mol percent Mg-perovskite with respect to a pyrolitic compositional model) (Figures 9–10). Despite the absence of quantitative information on the effect of the spin transition of Fe on the elastic properties of (Mg, Fe, Al)SiO_3 perovskite, we infer that the effect of a progressive spin transition across a broad pressure range is likely to require a revision of the thermal, compositional and mineralogical models of the lowermost mantle, toward hotter and more Si-depleted values than the upper part of the mantle.

4. Conclusions

[29] Based on our results, the Fe spin transition in magnesiowüstite appears to have an impact on the properties of the lower mantle that is comparable to that of the polymorphic transition of (Mg, Fe, Al)SiO_3 from perovskite to post-perovskite phase. Experiments documenting a close approach to quasi-equilibrium conditions, and a better understanding of the thermodynamics of the high-spin to low-spin transition in the FeO – MgO system are needed to better clarify the details of this electronic transition of Fe at lower mantle conditions.

[30] **Acknowledgments.** This research was supported by the University of California and the U.S. National Science Foundation. We thank E. K. Graham (Pennsylvania State University) for supplying sample material. We acknowledge the use of the facilities of beamline 12.2.2 at the Advanced Light Source, Lawrence Berkeley National Laboratory, and those of the GeoSoilEnviro-Consortium (GSECARS) and the High-Pressure Collaborative Access Team (HPCAT) at the Advanced Photon Source, Argonne National Laboratory. The Advanced Light Source is supported by the Director, Office of Science, Office of Basic Energy Sciences, Materials Sciences Division, of the U.S. Department of Energy under Contract No. DE-AC03-76SF00098 at Lawrence Berkeley National Laboratory. GSECARS is supported by the NSF, DOE, and the State of Illinois. HPCAT is supported by DOE-BES, DOE-NNSA (CDAC), NSF, DOD-TACOM, and the W.M. Keck Foundation. Use of APS was supported by the U.S. DOE-S, DOE-BES.This research has been supported by the U.S. Department of Energy and the University of California. This work, in collaboration with J.F.L. was performed under the auspices of the U.S. DOE by University of California and LLNL under Contract No. W-7405-Eng-48. J.F.L. is also supported by the Lawrence Livermore Fellowship. S.S. has been supported by the Miller Institute for basic Research in Science. S.S. thanks S. Jahn, M. Gottschalk, H. J. Reichmann and F. Schilling for very helpful discussions about the subject of this manuscript.

References

Badro, J., G. Fiquet, and F. Guyot (2005), Thermochemical state of the lower mantle. New insights from mineral physics, in *Earth's Deep Mantle: Structure, Composition, and Evolution*, edited by R. D. van der Hilst, J. D. Bass, J. Matas, and J. Trampert, pp. 241–260, Geophysical Monographs Series 160, AGU, Washington D. C., doi:10.1029/160GM15.

Badro, J., V. V. Struzhkin, J. Shu, R. J. Hemley, and H. K. Mao (1999), Magnetism in FeO at megabar pressures from x-ray emission spectroscopy, *Phys. Rev. Lett.*, *83*, 4101–4104.

Badro, J., G. Fiquet, F. Guyot, J.-P. Rueff, V. V. Struzhkin, G. Vankó, and G. Monaco (2003), Iron partitioning in Earth's mantle: Towards a deep lower mantle discontinuity, *Science*, *300*, 789–791.

Bonczar, L. J., and E. K. Graham (1982), The pressure and temperature dependence of the elastic properties of polycrystal magnesiowü stite, *J. Geophys. Res.*, *87*, 1061–1078.

Brown, J. M., and T. J. Shankland (1981), Thermodynamic parameters in the Earth as determined from seismic profiles, *Geophys. J. R. Astron. Soc.*, *66*, 579–596.

Burns, R. G. (1970), *Mineralogical Applications of Crystal Field Theory*, Cambridge Univ. Press, Cambridge UK.

Cohen, R. E., I. I. Mazin, and D. J. Isaak (1997), Magnetic collapse in transition metal oxides at high pressure: Implications for the Earth, *Science*, *275*, 654–657.

Dewaele, A., G. Fiquet, D. Andrault, and D. Hausermann (2000), P-V-T equation of state of periclase from synchrotron radiation measurements, *J. Geophys. Res.*, *105*, 2869–2877.

Dubrovinsky, L. S., N. A. Dubrovinskaya, H. Annersten, E. Hålenius, H. Harryson, F. Tutti, S. Rekhi, and T. LeBihan (2000), Stability of ferropericlase in the lower mantle, *Science*, *289*, 430–432.

Dziewonski, A. M., and D. L. Anderson (1981), Preliminary reference Earth model, *Phys. Earth Planet. Inter.*, *25*, 297–356.

Fei, Y. (1999), Effects of temperature and composition on the bulk modulus of (Mg, Fe)O, *Am. Mineral.*, *84*, 272–276.

Fei, Y., H. K. Mao, J. Shu, and J. Hu (1992), P-V-T equation of state of magnesiowüstite ($Mg_{0.6}Fe_{0.4}$)O, *Phys. Chem. Minerals*, *18*, 416–422.

Fei, Y., L. Zhang, A. Corgne, H. C. Watson, G. Shen, and V. B. Prakapenka (2005), Spin transition in (Mg, Fe)O at high pressure, *Eos Trans. AGU*, *86*(52), Fall Meet. Suppl., Abstract MR14A-05.

Fyfe, W. S. (1960), The possibility of d-electron coupling in olivine at high pressure, *Geochim. Cosmochim. Acta*, *19*, 141–143.

Gaffney, E. S., and D. L. Anderson (1973), Effect of low-spin Fe^{2+} on the composition of the lower mantle, *J. Geophys. Res.*, *78*, 7005–7014.

Goncharov, A. F., V. V. Struzhkin, and S. D. Jacobsen (2006), Reduced radiative conductivity of low-spin (Mg, Fe)O in the lower mantle, *Science*, *312*, 1205.

Hofmeister, A. M. (2006), Is low-spin Fe^{2+} present in Earth's mantle?, *Earth Planet. Sci. Lett.*, *243*, 44–52.

Jackson, I. (1998), Elasticity, composition and temperature of the Earth's lower mantle: a reappraisal, *Geophys. J. Int.*, *134*, 291–311.

Jackson, I., and H. Niesler (1982), The elasticity of periclase to 3 GPa and some geophysical implications, in *High Pressure Research in Geophysics*, edited by S.-I. Akimoto and M. Manghnani, pp. 93–114, Cent. For Acad. Publish. of Jp., Tokyo.

Jackson, I., and S. M. Rigden (1996), Analysis of P − V − T data: Constraints on the thermoelastic properties of high-pressure minerals, *Phys. Earth Planet. Inter.*, *96*, 85–112.

Jackson, I., R. C. Liebermann, and A. E. Ringwood (1978), The elastic properties of $(Mg_xFe_{1-x})O$ solid solutions, *Phys. Chem. Miner.*, *3*, 11–31.

Jackson, J. M., J. Zhang, and J. D. Bass (2004), Sound velocity and elasticity of aluminous $MgSiO_3$ perovskite: Implications for aluminum heterogeneityin Earth's lower mantle, *Geophys. Res. Lett.*, *31*, L10614, doi:10.1029/2004GL019918.

Jacobsen, S. D., H.-J. Reichmann, H. A. Spetzler, S. J. Mackwell, J. R. Smyth, R. J. Angel, and C. A. McCammon (2002), Structure and elasticity of single-crystal (Mg, Fe)O and a new method of generating shear waves for gigahertz ultrasonic interferometry, *J. Geophys. Res.*, *107*(B2), 2037, doi:10.1029/2001JB000490.

Jacobsen, S. D., J.-F. Lin, R. J. Angel, G. Shen, V. B. Prakapenka, P. Dera, H. K. Mao, and R. J. Hemley (2005), Single-crystal synchrotron x-ray diffraction study of wüstite and magnesiowüstite at lower mantle pressures, *J. Synchrotron Rad.*, *12*, 577–583.

Jeanloz, R. (1981), Finite-strain equation of state for high-pressure phases, *Geophys. Res. Lett.*, *8*, 1219–1222.

Kantor, I. Y., L. S. Dubrovinsky, and C. A. McCammon (2005), Spin transition in ferropericlase at high pressures and temperatures: Mössbauer spectroscopic study, *Eos Trans. AGU*, *86*(52), Fall Meet. Suppl., Abstract MR23A-0038.

Kantor, I. Yu., L. S. Dubrovinsky, and C. A. McCammon (2006a), Spin crossover in (Mg, Fe)O: A Mössbauer effect study with an alternative interpretation of x-ray emission spectroscopy data, *Phys. Rev. B*, *73*, 100101.

Kantor, I., L. S. Dubrovinsky, and C. A. McCammon (2007), Reply to "Comments on 'Spin crossover in (Mg, Fe)O: A Mössbauer effect study with an alternative interpretation of x-ray emission spectroscopy data'", *Phys. Rev. B*, *75*, 177103, doi:10.1103/PhysRevB.75.177103.

Kantor, I. Y., L. S. Dubrovinsky, C. A. McCammon, A. Kantor, S. Pascarelli, G. Aquilanti, W. Crichton, M. Mattesini, R. Ahuja, J. Almeida, and V. Ursov (2006b), Pressure-induced phase transition in $Mg_{0.8}Fe_{0.2}O$ ferropericlase, *Phys. Chem. Minerals*, doi:10.1007/ss00269-005-0052-z.

Kennett, B. L. N., E. R. Engdahl, and R. Buland (1995), Constraints on seismic velocities in the Earth from travel times, *Geophys. J. Int.*, *122*, 108–124.

Keppler, H., I. Kantor, and L. S. Dubrovinsky (2007), Optical absorption spectra of ferropericlase to 84 GPa, *Am. Mineral.*, *92*, 433–436.

Kondo, T., E. Ohtani, N. Hirao, T. Yagi, and T. Kikegawa (2004), Phase transition of (Mg, Fe)O at high pressures, *Phys. Earth Planet. Inter.*, *143–144*, 201–213.

Kunz, M., A. A. MacDowell, W. A. Caldwell, D. Cambie, R. S. Celestre, E. E. Domning, R. M. Duarte, A. E. Gleason, J. M. Glossinger, N. Kelez, D. W. Plate, T. Yu, J. M. Zaug, H. A. Padmore, R. Jeanloz, A. P. Alivizatos, and S. M. Clark (2005), A beamline for high pressure studies at the Advanced Light Source with a superconducting bending magnet as the source, *J. Synch. Rad.*, *12*, 650–658.

Lee, K. M., B. O'Neill, W. R. Panero, S.-H. Shim, L. R. Benedetti, and R. Jeanloz (2004), Equations of state of the high-pressure phases of a natural peridotite and implications for the Earth's lower mantle, *Earth Planet. Sci. Lett.*, *223*, 381–393.

Lin, J.-F., D. L. Heinz, H. K. Mao, R. J. Hemley, J. M. Devine, J. Li, and G. Shen (2003), Stability of magnesiowüstite in Earth's lower mantle, *Proc. Natl. Acad. Sci.*, *100*, 4405–4408.

Lin, J.-F., V. V. Struzhkin, S. D. Jacobsen, M. Y. Hu, P. Chow, J. Kung, H. Liu, H. K. Mao, and R. J. Hemley (2005), Spin transition of iron in magnesiowüstite in the Earth's lower mantle, *Nature*, *436*, 377–380.

Lin, J.-F., A. G. Gavriliuk, V. V. Struzhkin, S. D. Jacobsen, W. Sturhahn, M. J. Hu, P. Chow, and C.-S. Yoo (2006a), Pressure-induced spin transition of iron in magnesiowüstite- (Mg, Fe)O, *Phys. Rev. B*, *73*, 113107, doi:10.1103/PhysRevB.73.113107.

Lin, J.-F., S. D. Jacobsen, W. Sturhahn, J. M. Jackson, J. Zhao, and C.-S. Yoo (2006b), Sound velocities of ferropericlase in the Earth's lower mantle, *Geophys. Res. Lett.*, *33*, L22304, doi:10.1029/2006GL028099.

Lin, J.-F., S. D. Jacobsen, W. Sturhahn, J. M. Jackson, J. Zhao, and C.-S. Yoo (2007a), Correction to "Sound velocities of ferropericlase in the Earth's lower mantle", *Geophys. Res. Lett.*, *34*, L09301, doi:10.1029/2007GL029880.

Lin, J.-F., V. V. Struzhkin, A. G. Gavriliuk, and I. Lyubutin (2007b), Comment on "Spin crossover in (Mg, Fe)O: A Mössbauer effect study with an alternative interpretation of x-ray emission spectroscopy data", *Phys. Rev. B*, *75*, 177102.

Mao, W., J. Shu, R. J. Hemley, and H. K. Mao (2002), Displacive transition in magnesiowüstite, *J. Phys. Condens. Matter*, *14*, 11,349–11,354.

Marton, F., and R. E. Cohen (2002), Constraints on the lower mantle composition from molecular dynamics simulations of $MgSiO_3$ perovskite, *Phys. Earth Planet. Inter.*, *134*, 239–252.

Mattern, E., J. Matas, Y. Ricard, and J. Bass (2005), Lower mantle composition and temperature from mineral physics and thermodynamic modeling, *Geophys. J. Int.*, *160*, 973–990.

Murakami, M., K. Hirose, K. Kawamura, N. Sata, and Y. Ohishi (2004), Post-perovskite phase transition in $MgSiO_3$, *Science*, *304*, 855–858.

Oganov, A. R., and S. Ono (2004), Theoretical and experimental evidence for a post-perovskite phase of $MgSiO_3$ in Earth's D″ layer, *Nature*, *430*, 445–448.

Pasternak, M. P., R. D. Taylor, R. Jeanloz, X. Li, J. H. Nguyen, and C. A. McCammon (1997), High pressure collapse of magnetism in $Fe_{0.94}O$: Mössbauer spectroscopy beyond 100 GPa, *Phys. Rev. Lett.*, *79*, 5046–5049.

Persson, K., A. Bengtson, G. Ceder, and D. Morgan (2006), Ab initio study of the composition dependence of the pressure-induced spin transition in the $(Mg_{1-x}Fe_x)O$ system, *Geophys. Res. Lett.*, *33*, L16306, doi:10.1029/2006GL026621.

Richet, P., H. K. Mao, and P. M. Bell (1989), Bulk moduli of magnesiowüstites from static compression measurements, *J. Geophys. Res.*, *94*, 3037–3045.

Shannon, R. D., and C. T. Prewitt (1969), Effective ionic radii in oxides and fluorides, *Acta Crystallogr., B*, *25*, 925–946.

Sherman, D. M. (1988), High-spin to low-spin transition of iron (II) oxides at high pressures: Possible effects on the physics and chemistry of the lower mantle, in *Structural and Magnetic Phase Transitions in Minerals*, edited by S. Ghose, J. M. D. Coey, and E. Salje, pp. 113–128, Springer-Verlag, New York.

Shim, S.-H., T. S. Duffy, and G. Shen (2000), The equation of state of CaSiO3 perovskite to 108 GPa at 300 K, *Phys. Earth Planet. Inter.*, *120*, 327–338.

Shim, S.-H., T. S. Duffy, R. Jeanloz, and G. Shen (2004), Stability and crystal structure of $MgSiO_3$ perovskite to the core-mantle boundary, *Geophys. Res. Lett.*, *31*, L10603, doi:10.1029/2004GL019639.

Speziale, S., C.-S. Zha, T. S. Duffy, R. J. Hemley, and H. K. Mao (2001), Quasi-hydrostatic compression of magnesium oxide to 52 GPa: Implications for the pressure-volume-temperature equation of state, *J. Geophys. Res.*, *106*, 515–528.

Speziale, S., A. Milner, V. E. Lee, S. M. Clark, M. P. Pasternak, and R. Jeanloz (2005), Iron spin transition in Earth's mantle, *Proc. Natl. Acad. Sci. USA*, *102*, 17,918–17,922.

Struzhkin, V. V., H.-K. Mao, J. Hu, M. Schwoerer-Böhning, J. Shu, and R. J. Hemley (2001), Nuclear inelastic X-ray scatteringof FeO to 48 GPa, *Phys. Rev. Lett.*, *87*, 255501, doi:10.1103/PhysRevLett.87.255501.

Sturhahn, W., J. M. Jackson, and J.-F. Lin (2005), The spin state of iron in minerals of Earth's lower mantle, *Geophys. Res. Lett.*, *32*, L12307, doi:10.1029/2005GL022802.

Tsuchiya, T., R. M. Wentzcovitch, C. R. S. da Silva, and S. de Gironcoli (2006), Spin transition in magnesiowüstite in Earth's lower mantle, *Phys. Rev. Lett.*, *96*, 198501.

Vanpeteghem, C. B., J. Zhao, R. J. Angel, N. L. Ross, and N. Bolfan-Casanova (2006), Crystal structure and equation of state of MgSiO3 perovskite, *Geophys. Res. Lett.*, *33*, L03306, doi:10.1029/2005GL024955.

van Westrenen, W., J. Li, Y. Fei, M. R. Frank, H. Hellwig, T. Komabayashi, K. Mibe, W. G. Minarik, J. A. Van Orman, H. C. Watson, K.-I. Funakoshi, and M. W. Schmidt (2005), Thermoelastic properties of $(Mg_{0.64}Fe_{0.46})O$ ferropericlase based on in situ X-ray diffraction to 26.7 GPa and 2173 K, *Phys. Earth Planet. Inter.*, *151*, 163–176.

Weidner, D. J. (1994), Mantle model based on measured physical properties of minerals, in *Chemistry and Physics of Terrestrial Planets*, edited by S. K. Saxena, pp. 251–274, Springer Verlag, New York.

Wentzcovitch, R. M., B. B. Karki, M. Cococcioni, and S. de Gironcoli (2004), Thermoelastic properties of MgSiO3 perovskite: Insights on the nature of the Earth's lower mantle, *Phys. Rev. Lett.*, *92*, 018501.

Williams, E. J. (1935), The effect of thermal agitation on atomic arrangement in alloys III, *Proc. R. Soc. London, Ser. A*, *152*, 231–252.

S. M. Clark, Advanced Light Source, Lawrence Berkeley National Laboratory, Berkeley, CA 94720, USA.

R. Jeanloz and V. E. Lee, Department of Earth and Planetary Science, University of California, Berkeley, CA 94720, USA.

J. F. Lin, Lawrence Livermore National Laboratory, 7000 East Avenue, Livermore, CA 94550, USA.

M. P. Pasternak, School of Physics and Astronomy, Tel Aviv University, 69978 Tel Aviv, Israel.

S. Speziale, GeoForschungsZentrum Potsdam, Telegrafenberg, 9, 14473 Potsdam, Germany. (speziale@gfz-potsdam.de)